Advances in Science and Technology
ISSN: 1662-0356, Vol. 172, pp 267-275
doi:10.4028/p-JDf0Mt

Submitted: 2025-09-29
Accepted: 2025-11-05
Online: 2026-01-28

Mixed Electromagnetic Crack-Face Conditions in a Piezoelectric/Piezomagnetic Bimaterial under Antiplane Mechanical Loading and In-Plane Electric Fields

ONOPRIIENKO Oleg[1,a*], KAGADIY Tetiana[2,b] and SHPORTA Anna[2,c]

[1]Dnipro State Agrarian and Economic University, Dnipro, Ukraine

[2]Dnipro University of Technology, Dnipro, Ukraine

[a]onopriienko.o.d@dsau.dp.ua, [b]tkagadiy@gmail.com, [c]shporta.a.h@nmu.one

Keywords: fiber-reinforced composite, stress-strain state, perturbation method, contact stresses, fracture mechanics.

Abstract. An interface crack between two semi-infinite piezoelectric/piezomagnetic media under out-of-plane mechanical load and in-plane electric and magnetic fields parallel to the crack faces is examined. A portion of the faces is electrically conducting and kept at a uniform magnetic potential, while the remaining portion is electrically and magnetically permeable. The coupled fields are represented by functions analytic in the plane outside the crack. With these representations, the mixed crack-face conditions lead to a combined Dirichlet–Riemann and Hilbert boundary-value problem, which is solved in closed form for arbitrary conductive versus permeable segment lengths. The solution yields explicit expressions for stresses, electric and magnetic fields, and the crack-face sliding (displacement jump). The singular behavior at both crack tips and at the transition between conducting and permeable zones is characterized, and intensity factors are defined accordingly. Parametric results illustrate how applied electric and magnetic fields modulate the fracture driving force; in particular, suitable magnetic loading can markedly reduce the mechanical stress intensity at the permeable tip. The formulas supply benchmark data for verification and enable design guidelines for tailoring electrode coverage and field application to mitigate interface fracture. The approach provides an analytic framework for mixed electromagnetic conditions in magnetoelectroelastic interface fracture.

Introduction

Piezoelectric and magneto-electro-elastic solids are widely used in sensors, actuators, and layered smart structures, where brittle failure often initiates at bonded interfaces. Early fracture studies for piezoelectric media established the governing field couplings and highlighted the role of interface defects in electro-active ceramics [1]. Foundational analytical tools for cracks, inclusions, and dislocations in such materials provided the basis for mixed-field formulations used today [2]. Classical bi-material crack mechanics clarified near-tip fields and solution strategies for dissimilar media, which remain essential when an electromechanical coupling is present [3]. Further developments quantified stress distributions for bonded layers with cracks and offered benchmark configurations for validation [4]. The oscillatory character of certain interface singularities was first identified in purely elastic settings and motivates special care when extending to coupled problems [5].

Idealized crack-face conditions have been proposed to represent different gap fillings and surface treatments. The electrically permeable model allows normal electric flux to pass without free charge accumulation and is a standard baseline for piezoelectric fracture [1]. The electrically impermeable model treats the faces as insulating and is appropriate for dry, nonconducting gaps in ceramics [6]. A limited-permeability variant captures finite permittivity in the crack gap and bridges the two extremes used in practice [7]. For magnetoelectroelastic bimaterials, antiplane interface formulations and exact solution routes have been reported, enabling systematic study of coupled boundary choices [8]. Closed-form expressions for antiplane interface cracks in layered magnetoelectroelastic systems further demonstrate the tractability of such problems under realistic loading paths [9].

A distinctive feature of fully conducting interface configurations under antiplane shear with in-plane electric excitation is an oscillatory tip singularity, which complicates interpretation of near-tip fields and crack-face separation [9]. The origin of this behavior aligns with the oscillatory bi-material singularity known from elasticity and thus calls for remedies that restore physical admissibility [5]. One established approach is to allow a small contact or bonding zone at the tip, which regularizes the fields and eliminates nonphysical interpenetration in interface fracture [10]. Related contact-type and insulated-face treatments for piezoelectric bimaterials adapt this rationale to coupled electromechanical settings and guide practical boundary idealizations [11].

Beyond these paradigms, a wide literature explores geometry, coupling, and loading variants relevant to design and verification. Interfacial crack behavior in magnetoelectroelastic biomaterials reveals how coupling modifies singular trends and material selection [12]. Arrays and interactions of multiple interface cracks show sensitivity to spacing and anisotropy in layered piezoelectric composites [13]. Plane-strain studies for bounded magnetoelectroelastic layers with interfacial flaws document combined magneto-electro-mechanical effects under practical constraints [14]. Antiplane analyses for composite piezoceramic media provide additional reference solutions for benchmarking mixed-mode reductions [15]. Exact solutions for cracks and holes in piezoelectric plates clarify how geometry influences coupled fields and serve as checks for numerical schemes [16]. Thermally induced interfacial cracking demonstrates the interplay between thermal loads and coupled constitutive response in magnetoelectroelastic assemblies [17]. Dipole–crack interactions quantify how localized sources perturb interface singularities and inform transducer placement in smart structures [18]. Comprehensive treatments of interfacial cracks in magneto-electro-elastic solids synthesize these effects into unified frameworks suitable for engineering assessment [19]. Tension-field variants of the interface crack further delineate loading-path dependence and complement the standard shear-dominated cases used in antiplane formulations [20].

Against this background, the present work focuses on an interface crack whose faces are partly conducting and partly permeable, formulates the associated mixed boundary-value problem in a complex-variable setting, and derives closed-form results that expose how applied electric and magnetic fields can be used to tune the near-tip response and reduce fracture driving forces [4].

Methods

We consider a homogeneous piezo-electro-magnetic material (PEMM) occupying a half-space. In the linear constitutive form, the stress σ_{ij}, electric displacement D_i, and magnetic induction B_i are related to the strain S_{kl} (mechanical), electric field E_j and magnetic field H_j by:

$$\begin{aligned} \sigma_{ij} &= c_{ijks}\varepsilon_{ks} - e_{sij}E_s - h_{sij}H_s, \\ D_i &= e_{iks}\varepsilon_{ks} + \alpha_{is}E_s + d_{is}H_s, \\ B_i &= h_{iks}\varepsilon_{ks} + d_{is}E_s + \gamma_{is}H_s. \end{aligned} \tag{1}$$

which are the constitutive relations for a general magnetoelectroelastic (piezoelectromagnetic) medium. The equilibrium equations in the absence of body forces, free charges, or free currents are

$$\sigma_{ij,j} = 0,\ D_{i,i} = 0,\ B_{i,i} = 0. \tag{2}$$

and the strain–displacement and field–potential relations are:

$$\varepsilon_{ij} = \frac{1}{2}\left(u_{i,j} + u_{j,i}\right),\ E_i = -\varphi_{,i},\ H_i = -\psi_{,i}. \tag{3}$$

where $u_{i,j}$ is the mechanical displacement field, φ the electric potential, and ψ the magnetic potential.

In an antiplane case we have

$u_1 = u_2 = 0$, $u_3 = u_3(x_1, x_2)$, $\varphi = \varphi(x_1, x_2)$, $\psi = \psi(x_1, x_2)$.

Then, the constitutive relations take the form:

$\begin{Bmatrix} \sigma_{3i} \\ D_i \\ B_i \end{Bmatrix} = \mathrm{R} \begin{Bmatrix} u_{3,i} \\ -\varphi_{,i} \\ -\psi_{,i} \end{Bmatrix}$, where $i = 1,2$; $R = \begin{bmatrix} c_{44} & e_{15} & h_{15} \\ e_{15} & -\alpha_{11} & -d_{11} \\ h_{15} & -d_{11} & -\gamma_{11} \end{bmatrix}$.

Introducing the vectors

$$u = \left[u_3, \varphi, \psi\right]^T, t = \left[\sigma_{32}, D_2, B_2\right]^T, \tag{4}$$

one can write

$$t = Ru_{,2}. \tag{5}$$

As the functions u_3, φ and ψ are harmonic, then taking into account (5) the following presentations are valid:

$$\begin{aligned} u &= \Phi(z) + \overline{\Phi}(\overline{z}), \\ t &= B\Phi'(z) + \overline{B}\overline{\Phi}'(\overline{z}), \end{aligned} \tag{6}$$

where $\Phi(z) = \left[\Phi_1(z), \Phi_2(z), \Phi_3(z)\right]^T$ is an arbitrary analytical vector-function of the complex variable $z = x_1 + ix_2$, $B = iR$.

Problem Formulation

Geometry and Loading: We consider two dissimilar semi-infinite materials (material 1 for $y > 0$ and material 2 for $y < 0$) bonded along the interface $y = 0$ except for a crack occupying the interval $x \in [c,b]$ on the interface (Figure 1). One half $x \in [c,a]$ of the crack is assumed to have a thin compliant electrode and magnetic conductor bridging the faces, while the remaining half $x \in [a,b]$ has no such electrode. The crack surfaces are assumed to be traction-free (Mode III crack opens in shear). An out-of-plane shear stress and in-plane electric and magnetic fields are applied at infinity. Specifically, as $r \to \infty$, we impose a constant antiplane shear traction τ_∞ (so that $\sigma_{23} \to \tau_\infty$ on planes parallel to the interface), a uniform electric field E_∞ in the x_1-direction and a uniform magnetic field H_∞ in the x_1-direction . These loads are taken to be applied far from the crack and are self-balanced (no net charge or current input). A quasi-static, small-deformation setting is adopted, and each half-space is treated as homogeneous with fixed magneto-electro-elastic properties. The thin, compliant electrode on the left crack segment short-circuits the electric and magnetic potentials across the faces while adding negligible shear resistance. On the right segment the faces are electrically and magnetically permeable so field flux can pass through the gap; uniform far-field actions are prescribed to suppress edge effects and isolate the local response near the crack (Fig. 1). In addition, the transition point between the conducting and permeable segments marks where the boundary conditions change, and this interface edge effect is central to the field concentration discussed later. Outside the crack interval the bond is assumed perfect, so the two materials deform compatibly and transmit tractions and flux without slip or leakage. The remote loads are taken to be uniform and self-balanced, ensuring that the solution reflects the local behavior near the crack rather than artifacts from far boundaries.

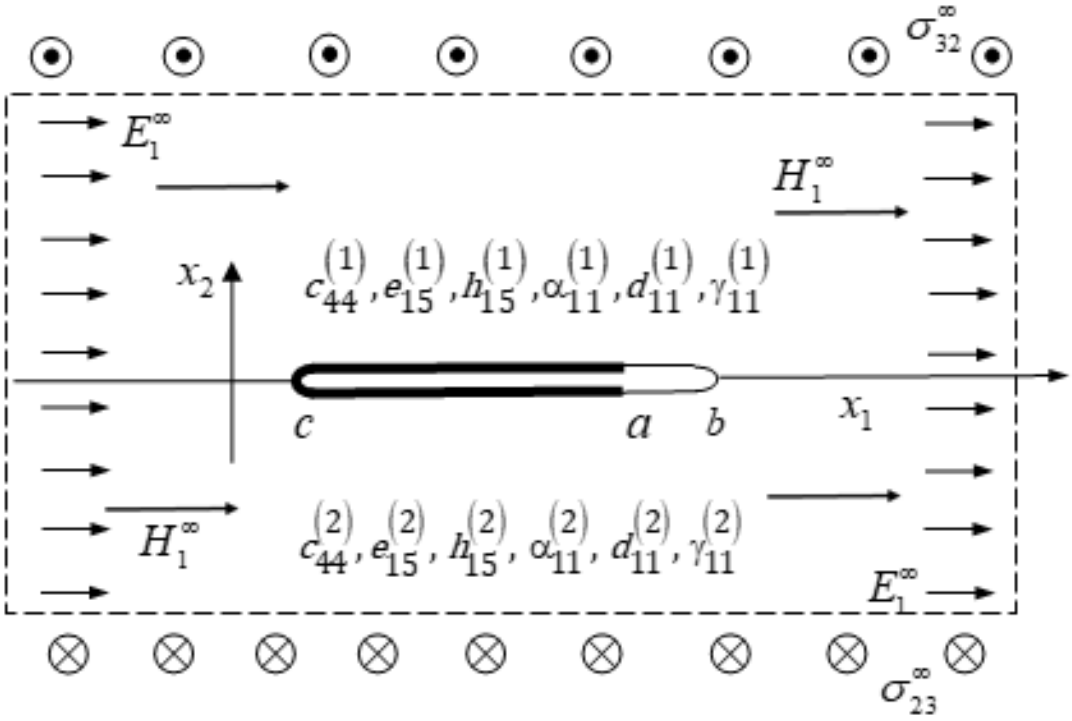

Fig. 1. A crack between two piezoelectromagnetic materials under out-of-plane mechanical load and in-plane electrical and magnetic fields

Boundary conditions on the crack faces: Because the crack is mode III, there is no opening in the normal direction; the two faces can slide relative to each other but remain in contact (no interpenetration). Hence, the crack faces at $x_2 = 0^{\pm}$ experience no normal traction or pressure. Along the conductive portion of the crack $x_1 \in [c, a]$, the electrode forces the electric potential to be equal on both faces and likewise enforces a constant magnetic potential. We take these potentials to be equal (and for convenience, zero reference) on the two crack faces. Thus, on $[c, a]$ one has

$$\sigma_{23}^{(1)} = \sigma_{23}^{(2)} = 0,\ E_1^{(1)} = E_1^{(2)} = 0,\ H_1^{(1)} = H_1^{(2)} = 0 \ \textit{for}\ c < x_1 < a \tag{7}$$

Along the permeable (non-electroded) portion of the crack the faces are insulating and no free charge or magnetic monopole exists on them. Therefore, this segment is modeled as electrically and magnetically permeable. The conditions are

$$\sigma_{32}^{(1)} = \sigma_{32}^{(2)} = 0, \langle D_2 \rangle = 0, \langle B_2 \rangle = 0, \langle E_1 \rangle = 0, \langle H_1 \rangle = 0 \ \textit{for}\ a < x_1 < b \tag{8}$$

In the above, superscripts (Eq.1) and (Eq.2) denote the upper and lower material, and x_2 -direction is the interface normal. It is worth noting that electrically permeable here means the crack gap does not restrict the normal electric flux unlike an impermeable gap which would enforce $\langle D_2 \rangle = 0$ on each face. Since our crack has no physical gap in the normal direction continuity of D_2 and B_2 is a reasonable condition for the open interface; effectively, the fields can pass through the interface as if it were unbroken, except for the discontinuity in material properties.

Continuity on the bonded interface. For $x < c$ and $x > b$ the interface is intact, so displacements and potentials are continuous and tractions/normal fluxes transmit between the two materials:

$[u3]=[\varphi]=[\psi]=0,\ \sigma_{32}^{(1)}=\sigma_{32}^{(2)},\ D_2^{(1)}=D_2^{(2)},\ B_2^{(1)}=B_2^{(2)}.$

Using the analytic representation, introduce the upper–half–plane vector potential $\Phi^{(1)}(\zeta)\ with\ \zeta=x_1+iy$. The boundary values on $y=0$ encode the transmission conditions. Continuity outside the crack $(x_1\notin[c,b])$ gives $Q_i^{(1)+}(x_1)=Q_i^{(2)-}(x_1)$ for $i=1,2,3$ where $\mathrm{Q}=(u_3,\varphi,\psi)^{\bullet}$. With these identities and the traction/flux conditions, any discontinuity of the analytic fields is confined to the crack interval $[c,b]$. Let $\mathrm{v}'(x_1)=\mathrm{Q}_{,x_1}(x_1,0)=(u_{3,x_1},\varphi_{,x_1},\psi_{,x_1})^{\bullet}$ denote the vector of tangential derivatives along the interface, and write jumps across $x_2=0$ as $\langle..\rangle$. Then the interface relation between the jump of v' and the boundary values of the analytic potential takes the compact form

$$\langle v'(x_1)\rangle = D\Phi'^{(1)}(x_1+i_0)+\bar{D}\bar{\Phi}'^{(1)}(x_1-i_0) \tag{9}$$

where $\mathrm{D}\ and\ \overline{\mathrm{D}}$ are constant matrices determined by the material parameters, the overbar denotes complex conjugation, and $x_1\pm i_0$ indicate limits to the real axis from above/below.

Mixed conditions as a coupled BVP. On the electroded (conducting) crack segment $[c,a]$ the potential jumps vanish, i.e. $[\varphi]=[\psi]=0\ \ with\ \ \sigma_{32}=0$ on the faces; on the permeable segment $[a,b]$ the normal fluxes are continuous, i.e. $\langle D_2\rangle=\langle B_2\rangle=0$ (again with $\sigma_{32}=0$) along $x_2=0$. Taken together, (7) – (8) give a combined Dirichlet–Riemann problem on $[c,a]$ (conditions posed on the potentials) and a Hilbert (jump) problem on $[a,b]$ (conditions posed on the normal inductions). To decouple these mixed boundary data, introduce the auxiliary substitution at the transition point $x_1=a$

$$\mathrm{F}(\zeta)=\Phi(\zeta)+\frac{\mathrm{K}}{\zeta-a}, \tag{10}$$

where $\mathrm{F}(\zeta)$ is the (vector) analytic field representation, $\Phi(\zeta)$ is an auxiliary analytic vector function, and K is a constant vector chosen so that the boundary data reduce to the simpler form on each subinterval. The resulting Riemann–Hilbert problem has the standard crack-end square-root structure and admits a closed-form solution. By linearity of the governing equations, the full response is obtained as the superposition of three subproblems driven separately by τ_∞, E_∞, and H_∞.

Analytical solution for a partially electroded interface crack

We consider a bimaterial interface crack occupying $x_1\in[c,b]$ on $x_2=0$, with an electroded (conducting) segment $[c,a]$ and a permeable segment $[a,b]$. On $[c,a]$ the electric and magnetic potentials are equal on the two faces, while on $[a,b]$ the normal electric and magnetic inductions are continuous; in both segments the shear traction on the faces is zero. In the antiplane setting we work with the field vectors

$$\mathrm{Q}=(u_3,\varphi,\psi)^{\bullet},\qquad \mathrm{P}=(\sigma_{13},D_3,B_3)^{\bullet}, \tag{11}$$

and use the complex variable $\zeta = x_1 + iy$ to represent sectionally analytic potentials. Across $x_2 = 0$, jumps are denoted by $\langle .. \rangle$. The transmission between traction/flux jumps and tangential field gradients is written in compact vector form by relating $\langle \mathrm{v}'(x_1) \rangle$ with boundary values of an analytic vector function for the upper half-plane, where $\mathrm{v}' = \partial \mathrm{Q} / \partial x_1$.

The mixed crack-face conditions reduce to a combined Dirichlet–Riemann problem on the conducting part $[c, a]$ and a Hilbert-type jump problem on the permeable part $[a, b]$. To decouple these data, we introduce an auxiliary substitution at the transition point $x_1 = a$,

$$\mathrm{F}(\zeta) = \Phi(\zeta) + \frac{\mathrm{K}}{\zeta - a}, \tag{12}$$

with a constant vector K chosen so that the boundary data on each segment take a simple, uniform form. This yields a standard Riemann–Hilbert problem with the usual square-root crack-end structure. The far-field actions (remote shear τ_∞, in-plane electric field E_∞, and magnetic field H_∞ enter the solution through the asymptotic behavior of the analytic functions. The problem is solved in closed analytical form for arbitrary position of a between c and b.

In terms of interface fields, the resulting expressions are elementary and capture the correct endpoint behavior. In particular, the crack-face sliding (displacement jump)

$$[w](x_1) = u_3^{(1)}(x_1, 0) - u_3^{(2)}(x_1, 0) = \frac{2}{\kappa_1 + \kappa_2}\left[K_0 \sqrt{(x_1 - c)(b - x_1)} + \Theta(x_1)\right], \tag{13}$$

$$c < x_1 < b,$$

where $\kappa_{1,2}$ are the antiplane shear moduli of the two halves, K_0 is a load-dependent constant (collecting $\tau_\infty, E_\infty, H_\infty$), and $\Theta(x_1)$ is an algebraic particular term due to the electric/magnetic loading (vanishing when $E_\infty = H_\infty = 0$). The normal components of the electric and magnetic fields on the permeable part exhibit the expected square-root behavior at the endpoints:

$$D_2(x_1, 0), B_2(x_1, 0) \sim (x_1 - a)^{-1/2} \text{ as } x_1 \to a^+, \qquad \sim (b - x_1)^{-1/2} \text{ as } x_1 \to b^-, \tag{14}$$

and are finite away from these points, with amplitudes governed by the material constants and the ratio of the conducting and permeable lengths. The complete solution for P, Q along the interface follows by superposition of the purely mechanical, electric, and magnetic load cases.

Results & Discussion

We evaluate the closed-form fields along the interface $x_2 = 0$ for a bimaterial with an interface crack $x_1 \in [c, b]$. The electroded (conducting) part is $[c, a]$, the permeable part is $[a, b]$. Remote actions are an out-of-plane shear τ_∞ and in-plane fields E_∞ and H_∞ along x_1. Quantities of interest are the crack-face sliding

$$[w](x_1) = u_3^{(1)}(x_1, 0) - u_3^{(2)}(x_1, 0),$$

and the normal components on the permeable segment, $D_2(x_1,0)$ and $B_2(x_1,0)$. For clarity, we non-dimensionalize lengths by $L=b-c$ (so $x=(x_1-c)/L\in[0,1]$) and use the conducting fraction $\alpha=(a-c)/L\in(0,1)$. Representative results are illustrated for electric-only, magnetic-only, and combined loading (see Fig. 2–Fig. 4).

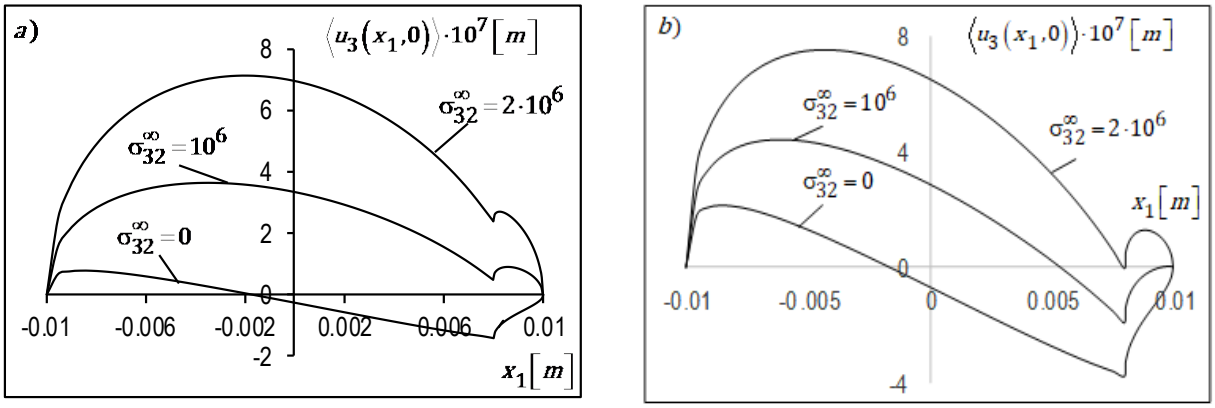

Fig. 2. The displacement jump at the segment $[c,b]$ for $E_1^{\infty}=9\cdot 10^3[V/m]$, $H_1^{\infty}=0$ (a) and $E_1^{\infty}=0$, $H_1^{\infty}=1.7\cdot 10^4[A/m]$ (b)

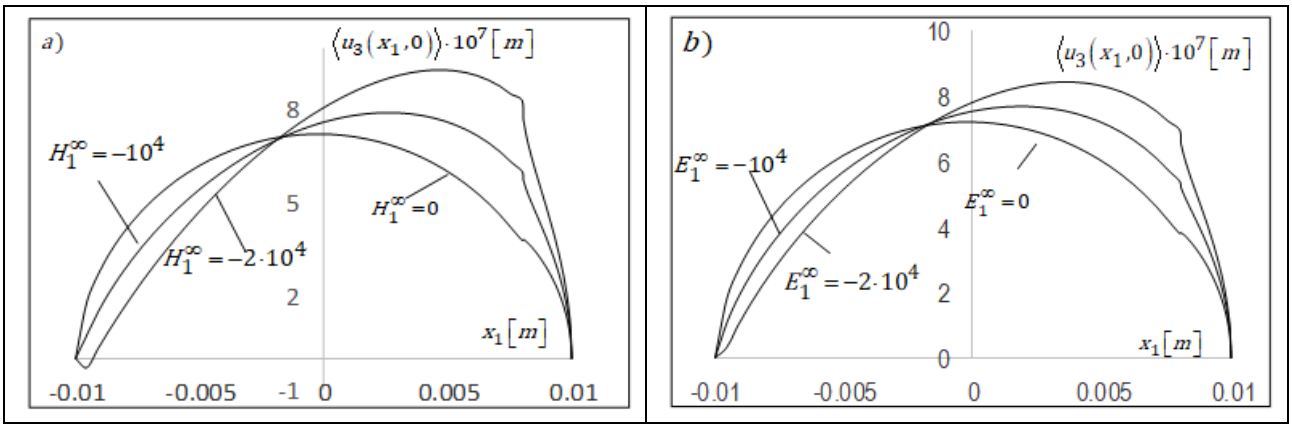

Fig. 3. The displacement jump at the segment $[c,b]$ for $\sigma^{\infty}=2\cdot 10^6\ Pa$ and different values of H^{∞} [*V/m*] and E^{∞} [*A/m*]

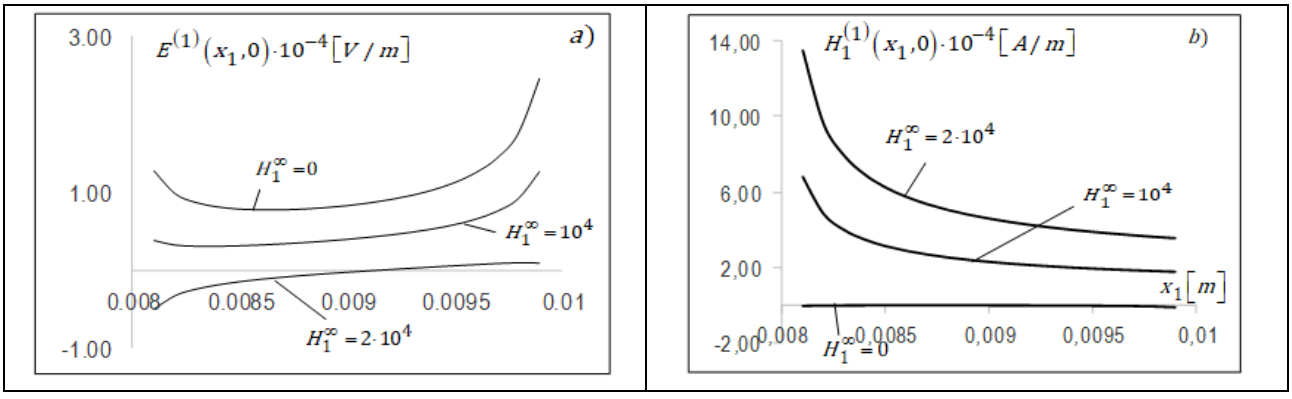

Fig.4. The variation of the electric $E_1^{(1)}(x_1,0)$ and magnetic $H_1^{(1)}(x_1,0)$ fields along the electro-magnetically permeable crack region (a,b)

Conclusions

An interface crack in a piezoelectric–piezomagnetic bimaterial under antiplane shear with in-plane electric and magnetic fields was examined with mixed crack-face conditions: an electroded (conducting) segment adjacent to a permeable segment. By employing sectionally analytic complex potentials and a transition-point substitution at the segment boundary, the mixed boundary data were reduced to a standard Dirichlet–Riemann/Hilbert formulation and solved in closed form. The solution delivers explicit interfacial field distributions and the crack-face sliding, and it clarifies the singularity structure: the mixed configuration suppresses nonphysical oscillations at the permeable tip and yields conventional square-root behavior at the segment endpoints, while any residual oscillation remains localized at the conducting tip and is admissible in antiplane shear.

Numerical evaluation confirmed the principal trends. Even without remote shear, applied electric or magnetic fields generate finite sliding through converse coupling, and the near-tip response is governed by the field magnitudes and the fraction of the crack covered by the electrode. Appropriately chosen magnetic loading and electrode coverage reduce the mechanical severity at the permeable tip, indicating a practical route to field-assisted mitigation of interfacial fracture in active layered structures.

References

[1] Adlucky, V. J., Levchenko, M. S., Loboda, V. V. (2024). Finite-element analysis of the parameters of fracture in a piezoelectric bimaterial with interface crack for various types of boundary conditions on its faces. *J. Math. Sci.*, 279, 181–196.

[2] Govorukha, V., Kamlah, M., Loboda, V., Lapusta, Y. (2016). Interface cracks in piezoelectric materials. *Smart Mater. Struct.*, 25(2), 023001.

[3] Lapusta, Y., Onopriienko, O., Loboda, V. (2017). An interface crack with partially electrically conductive crack faces under antiplane mechanical and in-plane electric loadings. *Mech. Res. Commun.*, 81, 38–43.

[4] Lei, J., Zhang, C., Bui, T. Q. (2015). Transient dynamic interface crack analysis in magnetoelectroelastic bimaterials by a time-domain BEM. *Eur. J. Mech. A/Solids*, 49, 146–157.

[5] Ma, P., Su, R. K. L., Feng, W. J. (2018). Singularity of subsonic and transonic crack propagations along interfaces of magnetoelectroelastic bimaterials. *Int. J. Eng. Sci.*, 129, 21–33.

[6] Rogowski, B. (2017). Exact solution for an anti-plane interface crack in piezoelectro-magneto-elastic bimaterials. *Arch. Appl. Mech.*, 87(6), 593–606.

[7] Shevelova, N., Khodanen, T., Chapelle, F., Lapusta, Y., Loboda, V. (2023). A set of collinear electrically charged interfacial cracks in magnetoelectroelastic bimaterial. *Acta Mech.*, 234(8), 4899–4915.

[8] Sulym, H. T., Piskozub, L. G., Piskozub, Y. Z., Pasternak, Y. M. (2015). Antiplane deformation of a bimaterial containing an interfacial crack with account of friction. I. Single loading. *Acta Mech. Autom.*, 9(2), 115–121.

[9] Sulym, H. T., Piskozub, L. G., Piskozub, Y. Z., Pasternak, Y. M. (2015). Antiplane deformation of a bimaterial containing an interfacial crack with account of friction. II. Repeating and cyclic loading. *Acta Mech. Autom.*, 9(3), 178–184.

[10] Tan, Y., Peng, F., Liu, C., Peng, D., Li, X. (2024). Fourth-order phase-field modeling for brittle fracture in piezoelectric materials. *Appl. Math. Mech. (Engl. Ed.)*, 45, 837–856.

[11] Tian, W., Zhong, Z., Li, Y. (2016). Multilayered piezomagnetic/piezoelectric composites with periodic interfacial cracks subject to in-plane loading. *Smart Mater. Struct.*, 25(1), 015029.

[12] Tian, X., Zhang, Y., Ma, H., Ding, X. (2024). Analysis of an interface crack between piezoelectric semiconductor coating and elastic substrate structure. *Mathematics*, 12(8), 1208.

[13] Yan, Z., Feng, W. J., Zhang, C., Liu, J. X. (2019). The extended finite element method with novel crack-tip enrichment functions for dynamic fracture analysis of interfacial cracks in piezoelectric-piezomagnetic bi-layered structures. *Comput. Mech.*, 64(5), 1303–1319.

[14] Yan, Z., Feng, W. J., Zhang, C. (2021). Interfacial crack growth in piezoelectric-piezomagnetic bi-layered structures with a modified mechanical energy release rate criterion. *Compos. Struct.*, 275, 113344.

[15] Yu, H., Zhu, S., Ma, H., Wang, J. (2024). Interface crack analysis of piezoelectric laminates considering initial strain. *Int. J. Mech. Sci.*, 271, 109104.

[16] Yu, T., Bui, T. Q., Liu, P., et al. (2015). Interfacial dynamic impermeable cracks analysis in dissimilar piezoelectric materials under coupled electromechanical loading with the extended finite element method. *Int. J. Solids Struct.*, 67–68, 205–218.

[17] Zhao, X., Liu, J. X., Qian, Z. H., Gao, C. F. (2019). Transient fracture of a piezoelectric-piezomagnetic sandwich structure: anti-plane case. *Acta Mech.*, 230(5), 1233–1246.

[18] Zhao, X., Qian, Z., Liu, J., Gao, C. (2020). Effects of electric/magnetic impact on the transient fracture of interface crack in piezoelectric-piezomagnetic sandwich structure: anti-plane case. *Appl. Math. Mech. (Engl. Ed.)*, 41(1), 139–156.

[19] Zhu, S., Yu, H., Wang, Z. (2025). Interfacial dynamic impermeable crack analysis in dissimilar piezoelectric materials by a new interaction integral. *Compos. Struct.*, 257, 118668.

[20] Viun, O., Loboda, V., Lapusta, Y. (2015). Periodic limited permeable cracks in magneto-electro-elastic media. *Acta Mech.*, 226(12), 2225–2233.